



STRUCTURAL  
BIOLOGY

**Volume 73 (2017)**

**Supporting information for article:**

**Factors affecting the amplitude of the  $\tau$  angle in proteins: a  
revisitation**

**Nicole Balasco, Luciana Esposito and Luigi Vitagliano**

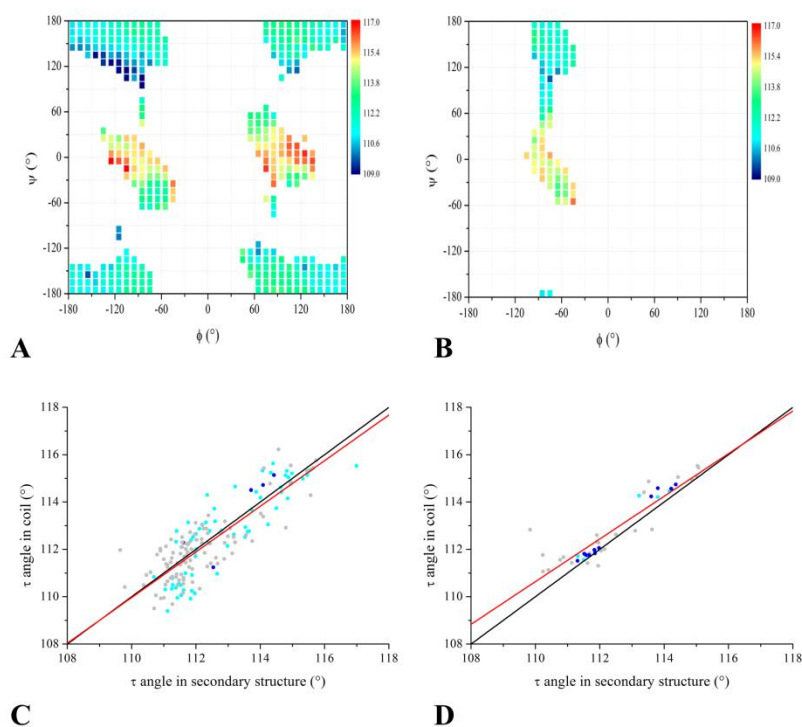


**Figure S1** Ramachandran plot highlighting the experimental dependence of the bond angle  $\tau$  on backbone conformation ( $\phi$ ,  $\psi$ ) for Gly (A) and Pro (B) residues. The values are calculated in the dataset Data1.6 by averaging the  $\tau$  angles in  $10^\circ \times 10^\circ$  ( $\phi$ ,  $\psi$ ) boxes. Only boxes containing at least 10 residues were considered. Since Gly and Pro display higher average  $\tau$  values than the other eighteen amino acid residues, the color scale is different (from  $109^\circ$  to  $117^\circ$ ) from that reported in Figure 1 (from  $107^\circ$  to  $115^\circ$ ). Correlation between the  $\tau$  values of the same ( $\phi, \psi$ ) boxes of residues belonging to secondary structure (H, E, P, or G) with those of residues of coil structures for Gly ( $R=0.81$ , regression line:  $y=1.11x+13$ ) (C) and Pro ( $R=0.93$ , regression line:  $y=0.91x+10$ ) (D). Regression lines and diagonals are in red and black, respectively. In panels C and D the data points have been colored using the scheme reported in the legend of Figure 2B. For Gly (C), the average values of the population of coil and secondary structure are 114 and 69 residues, respectively. For Pro (D), the average values of the population of coil and secondary structure are 330 and 206 residues, respectively.

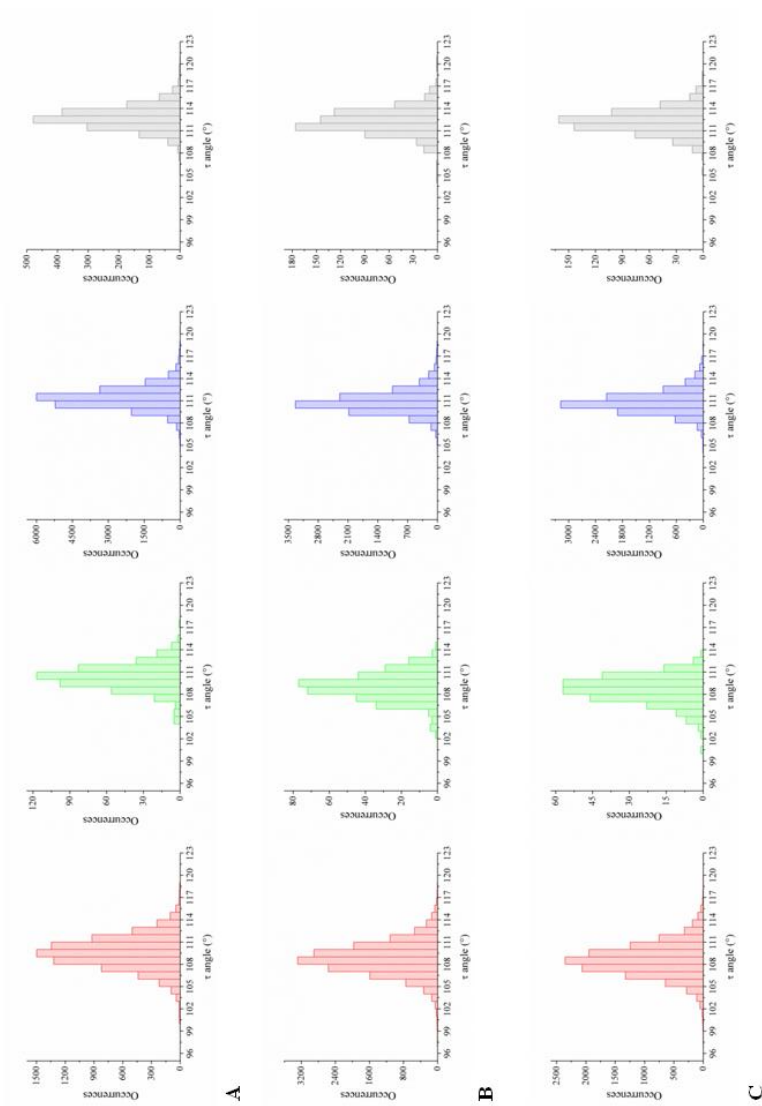


**Figure S2** Distributions of  $\tau$  values of Ala (A), Val (B), and Ile (C) residues in  $\beta$ -sheet (red), polyproline II (green),  $\alpha$ -helix (blue), and 3(10)-helix (grey) structures.

**Table S1** Average  $\tau$  values ( $^{\circ}$ ) with standard deviations and occurrences (in bracket) of amino acid residues in  $\alpha$ -helix, 3(10)-helix,  $\beta$ -sheet, and polyproline II structures.

Residue	$\alpha$ -helix	3(10)-helix	$\beta$ -sheet	polyproline II
A	111.4 $\pm$ 1.5 (19611)	112.7 $\pm$ 1.5 (1636)	109.6 $\pm$ 2.2 (7656)	110.3 $\pm$ 1.8 (454)
C	111.6 $\pm$ 1.6 (1732)	113.1 $\pm$ 1.5 (222)	109.7 $\pm$ 2.3 (1835)	110.5 $\pm$ 2.2 (61)
D	111.4 $\pm$ 1.6 (7763)	112.9 $\pm$ 1.6 (1408)	109.0 $\pm$ 2.5 (3747)	110.0 $\pm$ 1.9 (218)
E	111.5 $\pm$ 1.5 (13185)	112.7 $\pm$ 1.5 (1444)	109.4 $\pm$ 2.2 (5022)	110.0 $\pm$ 1.9 (260)
F	111.5 $\pm$ 1.8 (6605)	112.8 $\pm$ 1.7 (861)	109.4 $\pm$ 2.2 (7016)	110.4 $\pm$ 2.1 (133)
G	112.7 $\pm$ 1.8 (5536)	114.1 $\pm$ 1.9 (1117)	111.5 $\pm$ 2.3 (5861)	112.0 $\pm$ 1.6 (187)
H	111.9 $\pm$ 1.9 (3239)	113.0 $\pm$ 1.6 (507)	109.4 $\pm$ 2.3 (2773)	110.2 $\pm$ 2.2 (73)
I	110.8 $\pm$ 1.5 (9662)	112.2 $\pm$ 1.6 (604)	108.6 $\pm$ 2.2 (11486)	108.6 $\pm$ 1.8 (267)
K	111.4 $\pm$ 1.5 (9447)	112.7 $\pm$ 1.6 (1033)	109.3 $\pm$ 2.2 (4964)	110.1 $\pm$ 1.9 (312)
L	111.5 $\pm$ 1.6 (18905)	112.7 $\pm$ 1.5 (1649)	109.2 $\pm$ 2.3 (12146)	110.3 $\pm$ 1.8 (500)
M	111.6 $\pm$ 1.6 (3655)	112.7 $\pm$ 1.7 (302)	109.5 $\pm$ 2.2 (2170)	110.4 $\pm$ 1.9 (78)
N	111.6 $\pm$ 1.8 (5067)	113.3 $\pm$ 1.7 (924)	109.5 $\pm$ 2.5 (3194)	110.4 $\pm$ 2.1 (126)
P	113.6 $\pm$ 1.6 (3200)	114.2 $\pm$ 1.7 (1251)	111.5 $\pm$ 2.2 (2253)	111.8 $\pm$ 1.9 (1292)
Q	111.5 $\pm$ 1.5 (7579)	112.7 $\pm$ 1.5 (771)	109.4 $\pm$ 2.2 (3189)	110.2 $\pm$ 1.7 (170)
R	111.4 $\pm$ 1.5 (9322)	112.6 $\pm$ 1.7 (914)	109.3 $\pm$ 2.3 (5131)	110.3 $\pm$ 1.8 (247)
S	111.8 $\pm$ 1.6 (7000)	113.0 $\pm$ 1.6 (1347)	109.9 $\pm$ 2.2 (5960)	110.7 $\pm$ 1.9 (289)
T	111.4 $\pm$ 1.7 (7018)	112.7 $\pm$ 1.7 (790)	109.6 $\pm$ 2.2 (7972)	109.7 $\pm$ 2.1 (292)
V	110.8 $\pm$ 1.5 (10410)	112.2 $\pm$ 1.7 (668)	108.8 $\pm$ 2.2 (15807)	109.1 $\pm$ 1.9 (334)
W	111.5 $\pm$ 1.8 (2667)	112.9 $\pm$ 1.6 (461)	109.6 $\pm$ 2.3 (2435)	110.6 $\pm$ 2.3 (58)
Y	111.6 $\pm$ 1.8 (5851)	112.8 $\pm$ 1.6 (831)	109.6 $\pm$ 2.2 (6217)	110.0 $\pm$ 2.1 (137)

**Table S2** Difference between the average  $\tau$  values and p-values emerging from the comparison of the distribution described in Table 3.

Comparison	Difference	p-value
H vs C in 8°x8°-box centered at ( $\phi,\psi$ )=(-69°, -19°)	0.4°	5.2*10 <sup>-12</sup>
H vs C in 8°x8°-box centered at ( $\phi,\psi$ )=(-69°, -51°)	0.8°	1.5*10 <sup>-11</sup>
H in 8°x8°-box centered at ( $\phi,\psi$ )=(-69°, -19°) vs H in 8°x8°-box centered at ( $\phi,\psi$ )=(-69°, -51°)	1.8°	3.7*10 <sup>-281</sup>
E vs C in 15°x15°-box centered at ( $\phi,\psi$ )=(-112.5°, 112.5°)	0.7°	3.5*10 <sup>-24</sup>
E vs C in 15°x15°-box centered at ( $\phi,\psi$ )=(-97.5°, 142.5°)	0.5°	4.6*10 <sup>-19</sup>
E in 15°x15°-box centered at ( $\phi,\psi$ )=(-112.5°, 112.5°) vs E in 15°x15°-box centered at ( $\phi,\psi$ )=(-97.5°, 142.5°)	2.3°	0 (< 10 <sup>-300</sup> )

**Table S3** Average  $\tau$  values and occurrences (in bracket) of non-Gly/non-Pro residues in  $\alpha$ -helices or coil in  $5^\circ \times 5^\circ$ -boxes in the lower left quadrant of the Ramachandran plot.

The difference (coil minus  $\alpha$ -helix) between the average  $\tau$  values is reported .

<b><math>5^\circ \times 5^\circ</math>-box centered at (<math>\phi</math>;<math>\psi</math>)</b>	<b><math>\tau</math> angle in <math>\alpha</math>-helix (<math>^\circ</math>)</b>	<b><math>\tau</math> angle in coil (<math>^\circ</math>)</b>	<b>Difference (<math>^\circ</math>)</b>
-67.5, -47.5	110.8 (4504)	111.8 (166)	1.0
-62.5, -47.5	110.8 (13222)	111.8 (265)	1.0
-57.5, -47.5	110.9 (11120)	111.9 (205)	1.0
-67.5, -42.5	110.9 (11958)	111.9 (339)	1.0
-62.5, -42.5	111.0 (24994)	111.8 (420)	0.8
-57.5, -42.5	111.2 (11743)	111.9 (408)	0.7
-67.5, -37.5	111.3 (10758)	111.9 (386)	0.6
-62.5, -37.5	111.4 (13342)	111.9 (495)	0.5
-57.5, -37.5	111.6 (4408)	112.3 (460)	0.7

**Table S4** Average  $\tau$  values and occurrences (in bracket) of non-Gly/non-Pro residues in  $\beta$ -structure or coil in  $5^\circ \times 5^\circ$ -boxes in the upper left quadrant of the Ramachandran plot. The difference (coil minus  $\beta$ -sheet) between the average  $\tau$  values is reported.

$5^\circ \times 5^\circ$ -box centered at ( $\phi$ ; $\psi$ )	$\tau$ angle in $\beta$ -sheet ( $^\circ$ )	$\tau$ angle in coil ( $^\circ$ )	Difference ( $^\circ$ )
-122.5, 127.5	108.5 (1349)	108.5 (178)	0.0
-117.5, 127.5	108.6 (1370)	108.8 (176)	0.2
-112.5, 127.5	108.7 (1267)	109.0 (207)	0.3
-122.5, 132.5	108.9 (1333)	109.1 (195)	0.2
-117.5, 132.5	109.0 (1305)	109.3 (177)	0.3
-112.5, 132.5	108.9 (1148)	109.7 (203)	0.8
-122.5, 137.5	109.5 (1158)	109.5 (181)	0.0
-117.5, 137.5	109.4 (1041)	109.6 (193)	0.2
-112.5, 137.5	109.4 (886)	109.8 (172)	0.4

**Table S5** p-values obtained from the pairwise comparison of the distributions of the  $\tau$  angle of Ala, Val, and Ile residues in  $\alpha$ -helix, 3(10)-helix,  $\beta$ -sheet, and polyproline II structures.

	Ala vs Val	Ala vs Ile	Val vs Ile
<b>H</b>	$1.4 \times 10^{-213}$	$4.7 \times 10^{-220}$	0.35
<b>G</b>	$4.6 \times 10^{-11}$	$5.6 \times 10^{-11}$	0.92
<b>E</b>	$3.1 \times 10^{-144}$	$6.1 \times 10^{-203}$	$1.8 \times 10^{-14}$
<b>P</b>	$1.7 \times 10^{-20}$	$1.8 \times 10^{-30}$	0.0061

**Table S6** Average values of ( $\phi$ ,  $\psi$ ) angles ( $^{\circ}$ ) of the amino acid residues in  $\alpha$ -helix, 3(10)-helix,  $\beta$ -sheet, and polyproline II structures.

Residue	$\alpha$ -helix	3(10)-helix	$\beta$ -sheet	polyproline II
A	-63.4, -39.6	-64.4, -19.7	-122.0, 134.2	-69.8, 146.0
C	-65.5, -39.6	-69.1, -14.7	-121.7, 128.5	-76.7, 143.9
D	-64.1, -38.9	-69.9, -9.9	-104.4, 110.5	-72.1, 143.3
E	-64.7, -39.5	-69.9, -16.1	-114.9, 128.4	-75.1, 143.3
F	-66.0, -40.5	-76.7, -8.8	-119.9, 134.4	-77.0, 142.9
G	-59.5, -40.8	-21.4, -30.6	-122.3, 149.7*	-73.4, 157.7
H	-67.5, -38.6	-75.9, -7.9	-118.1, 129.2	-75.4, 143.4
I	-65.1, -42.2	-70.2, -19.5	-114.2, 123.8	-83.4, 130.9
K	-64.5, -39.6	-69.0, -15.3	-114.4, 129.2	-74.6, 141.4
L	-65.5, -39.3	-72.2, -16.9	-109.5, 123.3	-77.7, 143.8
M	-65.3, -38.7	-71.1, -13.1	-117.9, 130.4	-82.1, 139.0
N	-67.5, -35.9	-65.1, -2.7	-105.0, 115.9	-73.2, 146.4
P	-59.3, -35.5	-59.7, -20.5	-69.9, 137.5	-66.5, 149.9
Q	-64.9, -39.1	-72.3, -14.1	-116.2, 131.1	-78.4, 142.8
R	-64.5, -39.7	-69.3, -15.0	-116.8, 130.6	-75.7, 142.0
S	-65.5, -37.1	-67.2, -15.8	-123.1, 131.1	-73.1, 150.6
T	-67.4, -39.8	-73.0, -12.8	-118.6, 126.5	-79.3, 141.7
V	-65.3, -41.9	-71.6, -15.6	-116.5, 125.8	-81.1, 133.8
W	-64.9, -40.2	-66.9, -14.5	-126.8, 133.7	-80.1, 143.4
Y	-66.4, -40.0	-75.8, -7.4	-120.9, 135.4	-77.3, 140.6

\*The average value of Gly residues in  $\beta$ -sheet structures is calculated considering only the upper left quadrant of the Ramachandran plot.



**Table S7** Average  $\tau$  values ( $^{\circ}$ ) with standard deviations and occurrences (in bracket) of amino acid residues in  $\alpha$ -helix in the  $3^{\circ}\times 3^{\circ}$ -box centered at  $(\varphi,\psi)=(-63^{\circ},-43^{\circ})$  and in  $\beta$ -sheet in the  $15^{\circ}\times 15^{\circ}$ -box centered at  $(\varphi,\psi)=(-120^{\circ},130^{\circ})$ .

Box	$3^{\circ}\times 3^{\circ}$ centered at $(\varphi,\psi)=(-63^{\circ},-43^{\circ})$	$15^{\circ}\times 15^{\circ}$ centered at $(\varphi,\psi)=(-120^{\circ},130^{\circ})$
Residue	$\langle\tau\rangle \pm \sigma$ ( $^{\circ}$ )	$\langle\tau\rangle \pm \sigma$ ( $^{\circ}$ )
A	111.0 $\pm$ 1.1 (1546)	108.8 $\pm$ 2.1 (414)
C	111.1 $\pm$ 1.0 (95)	109.8 $\pm$ 2.1 (130)
D	110.9 $\pm$ 1.3 (439)	108.8 $\pm$ 2.1 (81)
E	111.1 $\pm$ 1.2 (838)	108.8 $\pm$ 2.0 (435)
F	110.8 $\pm$ 1.2 (265)	109.1 $\pm$ 1.8 (476)
G	112.1 $\pm$ 1.3 (338)	110.0 $\pm$ 2.2 (90)
H	111.2 $\pm$ 1.1 (167)	109.2 $\pm$ 1.8 (175)
I	110.5 $\pm$ 1.2 (640)	108.4 $\pm$ 1.9 (2044)
K	110.8 $\pm$ 1.1 (664)	108.7 $\pm$ 1.8 (398)
L	111.1 $\pm$ 1.2 (1105)	108.9 $\pm$ 2.0 (1195)
M	111.1 $\pm$ 1.3 (235)	108.9 $\pm$ 2.0 (180)
N	111.3 $\pm$ 1.2 (239)	109.1 $\pm$ 2.1 (132)
Q	111.0 $\pm$ 1.2 (524)	109.0 $\pm$ 1.9 (242)
R	111.0 $\pm$ 1.2 (564)	108.9 $\pm$ 2.0 (400)
S	111.3 $\pm$ 1.2 (340)	109.3 $\pm$ 2.1 (277)
T	110.7 $\pm$ 1.2 (395)	109.0 $\pm$ 2.0 (1034)
V	110.4 $\pm$ 1.1 (644)	108.6 $\pm$ 1.9 (2795)
W	110.9 $\pm$ 1.2 (137)	108.9 $\pm$ 2.0 (155)
Y	110.8 $\pm$ 1.3 (225)	109.0 $\pm$ 2.0 (473)

**Table S8** Average  $\tau$  values ( $^{\circ}$ ) with standard deviations and occurrences (in bracket) of amino acid residues in  $\alpha$ -helix in the  $8^{\circ}\times 8^{\circ}$ -boxes centered at  $(\phi,\psi)=(-69^{\circ},-19^{\circ})$  and  $(-69^{\circ},-51^{\circ})$  and in  $\beta$ -sheet in the  $15^{\circ}\times 15^{\circ}$ -boxes centered at  $(\phi,\psi)=(-112.5^{\circ},112.5^{\circ})$  and  $(-97.5^{\circ},142.5^{\circ})$ .

Residue	H		E	
	8°x8°-box centered at ( $\phi,\psi$ )		15°x15°-box centered at ( $\phi,\psi$ )	
	(-69°, -19°)	(-69°, -51°)	(-112.5°, 112.5°)	(-97.5°, 142.5°)
A	112.7 ± 1.3 (206)	111.1 ± 1.4 (207)	108.0 ± 1.8 (132)	110.1 ± 2.1 (273)
C	113.1 ± 1.2 (21)	111.0.8 ± 1.4 (34)	108.3 ± 1.9 (64)	110.2 ± 2.1 (57)
D	112.5 ± 1.3 (95)	110.9 ± 1.9 (91)	107.7 ± 2.2 (175)	109.5 ± 2.3 (107)
E	113.0 ± 1.4 (126)	111.1 ± 1.5 (176)	107.8 ± 2.0 (142)	110.0 ± 2.0 (188)
F	112.7 ± 1.3 (63)	110.8 ± 1.7 (185)	107.5 ± 2.1 (260)	110.1 ± 2.0 (311)
G	114.1 ± 1.4 (76)	112.4 ± 1.7 (85)	109.1 ± 1.9 (34)	111.4 ± 2.1 (157)
H	113.1 ± 1.4 (35)	111.0 ± 1.6 (62)	108.1 ± 2.1 (134)	110.0 ± 2.0 (92)
I	112.1 ± 1.3 (39)	110.5 ± 1.4 (390)	107.5 ± 1.8 (831)	109.4 ± 1.9 (198)
K	112.7 ± 1.2 (88)	111.2 ± 1.4 (120)	107.6 ± 2.2 (114)	109.9 ± 1.9 (136)
L	112.8 ± 1.3 (181)	111.1 ± 1.5 (343)	107.6 ± 1.9 (684)	110.0 ± 2.1 (521)
M	113.0 ± 1.3 (52)	110.8 ± 1.6 (65)	108.5 ± 2.2 (78)	110.3 ± 1.8 (75)
N	112.9 ± 1.2 (76)	111.8 ± 1.9 (51)	107.8 ± 2.0 (145)	110.2 ± 1.9 (107)
Q	112.7 ± 1.5 (70)	111.2 ± 1.4 (82)	107.8 ± 2.1 (78)	109.9 ± 2.1 (106)
R	112.5 ± 1.4 (108)	111.3 ± 1.5 (144)	107.6 ± 2.2 (145)	109.8 ± 2.3 (145)
S	112.7 ± 1.3 (185)	111.4 ± 1.5 (87)	107.7 ± 2.5 (107)	110.1 ± 2.1 (170)
T	112.4 ± 1.5 (53)	110.8 ± 1.3 (194)	108.0 ± 1.8 (195)	110.0 ± 2.1 (177)
V	112.6 ± 1.3 (29)	110.6 ± 1.4 (417)	107.5 ± 2.0 (850)	109.5 ± 2.1 (213)
W	113.0 ± 1.4 (33)	110.9 ± 1.6 (70)	108.1 ± 2.7 (79)	110.3 ± 2.0 (104)
Y	110.8 ± 1.3 (28)	109.0 ± 2.0 (154)	110.8 ± 1.3 (217)	109.0 ± 2.0 (215)

**Table S9** Average  $\tau$  values ( $^{\circ}$ ) with standard deviations and occurrences (in bracket) of amino acid residues in  $\alpha$ -helix or 3(10)-helix in the  $8^{\circ}\times 8^{\circ}$ -box centered at  $(\phi,\psi)=(-67.5^{\circ},-22.5^{\circ})$  and in  $\beta$ -sheet or polyproline II in the  $20^{\circ}\times 20^{\circ}$ -box centered at  $(\phi,\psi)=(-67.5^{\circ},142.5^{\circ})$ .

Residue	$8^{\circ}\times 8^{\circ}$ -box centered at $(\phi,\psi) = (-67.5^{\circ}, -22.5^{\circ})$		$20^{\circ}\times 20^{\circ}$ -box centered at $(\phi,\psi)=(-67.5^{\circ}, 142.5^{\circ})$	
	H	G	E	P
A	112.5 $\pm$ 1.2 (348)	112.5 $\pm$ 1.4 (110)	110.4 $\pm$ 1.7 (305)	110.6 $\pm$ 1.7 (191)
C	112.9 $\pm$ 1.5 (33)	112.7 $\pm$ 1.3 (15)	110.3 $\pm$ 2.1 (38)	110.3 $\pm$ 1.4 (18)
D	112.4 $\pm$ 1.4 (142)	112.6 $\pm$ 1.7 (72)	110.3 $\pm$ 1.9 (171)	110.1 $\pm$ 1.3 (57)
E	112.7 $\pm$ 1.6 (190)	112.6 $\pm$ 1.1 (110)	110.3 $\pm$ 1.8 (209)	110.0 $\pm$ 1.7 (77)
F	112.7 $\pm$ 1.3 (86)	112.6 $\pm$ 1.2 (48)	110.4 $\pm$ 1.9 (179)	110.5 $\pm$ 1.6 (45)
G	113.8 $\pm$ 1.6 (121)	114.1 $\pm$ 1.7 (59)	111.4 $\pm$ 1.8 (153)	111.6 $\pm$ 1.4 (57)
H	113.0 $\pm$ 1.4 (45)	112.9 $\pm$ 1.3 (22)	109.7 $\pm$ 1.9 (75)	110.6 $\pm$ 1.7 (24)
I	112.0 $\pm$ 1.4 (82)	112.1 $\pm$ 1.3 (55)	109.5 $\pm$ 1.7 (128)	109.0 $\pm$ 1.6 (40)
K	112.2 $\pm$ 1.4 (158)	112.5 $\pm$ 1.2 (65)	110.0 $\pm$ 1.8 (241)	110.0 $\pm$ 2.0 (87)
L	112.6 $\pm$ 1.2 (318)	112.4 $\pm$ 1.2 (98)	110.3 $\pm$ 1.9 (357)	110.6 $\pm$ 1.7 (138)
M	112.8 $\pm$ 1.4 (69)	112.4 $\pm$ 1.2 (22)	110.6 $\pm$ 1.7 (55)	110.8 $\pm$ 1.1 (16)
N	113.0 $\pm$ 1.4 (97)	113.3 $\pm$ 1.5 (45)	110.1 $\pm$ 1.7 (122)	110.6 $\pm$ 2.1 (36)
P	113.5 $\pm$ 1.2 (118)	113.8 $\pm$ 1.7 (74)	111.5 $\pm$ 2.0 (1101)	112.0 $\pm$ 1.7 (491)
Q	112.5 $\pm$ 1.2 (129)	112.5 $\pm$ 1.4 (61)	109.8 $\pm$ 1.7 (113)	110.5 $\pm$ 1.3 (39)
R	112.2 $\pm$ 1.4 (155)	112.1 $\pm$ 2.0 (58)	109.9 $\pm$ 2.1 (236)	110.3 $\pm$ 1.1 (71)
S	112.5 $\pm$ 1.3 (269)	112.7 $\pm$ 1.4 (124)	110.6 $\pm$ 1.8 (222)	111.1 $\pm$ 1.6 (76)
T	112.2 $\pm$ 1.5 (90)	112.3 $\pm$ 1.6 (65)	110.0 $\pm$ 1.6 (125)	109.9 $\pm$ 2.0 (49)
V	112.0 $\pm$ 1.3 (71)	112.3 $\pm$ 1.6 (52)	109.7 $\pm$ 1.8 (167)	109.6 $\pm$ 1.7 (67)
W	112.7 $\pm$ 1.3 (52)	112.9 $\pm$ 1.2 (36)	110.2 $\pm$ 2.1 (106)	110.5 $\pm$ 1.8 (20)
Y	112.8 $\pm$ 1.8 (59)	112.5 $\pm$ 1.6 (44)	110.3 $\pm$ 1.9 (139)	110.3 $\pm$ 1.8 (40)